

# Classification and Mapping of Mangrove Forest Area in Eastern Leyte Using Percentile-Based Threshold Segmentation

Sarah Jane L. Cabral<sup>1,2\*</sup>, Sarah Alma Bentir<sup>3</sup>, Jayson M. Victoriano<sup>3</sup>

<sup>1</sup>Faculty, Eastern Visayas State University, Tacloban Leyte Philippines

<sup>2</sup>DIT candidate, La Consolacion University Philippines, Malolos Bulacan Philippines

<sup>3</sup>Faculty, Bulacan State University, Malolos Bulacan Philippines

\*Corresponding Author: [sarahjane.cabral@evsu.edu.ph](mailto:sarahjane.cabral@evsu.edu.ph)

## ARTICLE INFO

Received: 30 Dec 2024

Revised: 12 Feb 2025

Accepted: 26 Feb 2025

## ABSTRACT

Mangroves in Eastern Leyte play an important role in the environment by offering various ecological benefits like protecting shorelines, storing carbon and serving as homes for a variety of marine creatures. It is crucial to map and monitor mangrove forests to properly conserve and manage them. This research study specifically looks at how to identify and locate mangrove areas in Eastern Leyte Philippines using satellite images. A method based on the 75th percentile threshold segmentation index was used to detect and classify these mangrove areas. Field surveys provided ground truth data to confirm the accuracy of the classification results, which showed an overall accuracy rate of 83.93% and a Kappa coefficient of 0.678 indicating substantial agreement between the classified information and the actual data. The high level of accuracy demonstrates that the percentile-based threshold segmentation method is reliable in distinguishing mangrove areas from types of land cover. This study offers an efficient and faster approach for mapping mangroves in Eastern Leyte that can be applied to ecological research in different locations. The outcomes support the development of management strategies, contribute to global initiatives aimed at protecting and conserving mangroves.

**Keywords:** Mangrove Area, Remote Sensing, Percentile-Thresholding, Sentinel-2A, Forecasting

## INTRODUCTION

Mangroves are more than just trees along the coastline; they are a vital part of the life and culture of Eastern Leyte, Philippines. These unique ecosystems, with their sprawling roots and vibrant canopies, offer a sanctuary for a variety of marine life, protect shores from storms, and provide resources that many local communities depend on for their livelihoods. For the people living in these coastal areas, mangroves are also a source of sustenance, offering fish, wood, other essential products and tourism. Mangroves have been suggested as a natural defense against coastal erosion, helping protect inland areas from natural disasters like typhoons, cyclones, and tsunamis [1]. Restoring mangroves for coastal protection is expected to be up to five times more cost-effective than building "grey infrastructure" like breakwaters [2].

However, the country is vulnerable to typhoons due to its geographic location in the Pacific Ocean continues to experience significant mangrove losses. Each year, an average of 20 tropical cyclones enters the Philippine Area of Responsibility (PAR), with around 8 or 9 making landfall [3]. One of the most catastrophic typhoons in history, Typhoon Haiyan, struck the country in 2013, damaging approximately 86% of the mangrove areas in Eastern Visayas [4]. This event highlighted the importance to monitor trends in mangrove distribution and dynamics in order to develop an effective conservation and management programs [5]. Analyzing mangrove distribution is crucial to assess and evaluate these natural ecosystems [6]. To effectively conserve and manage mangroves, tools and methods are needed to track spatiotemporal changes caused by both natural disasters and human activity.

Traditionally, mangrove ecosystems were monitored through field observations and surveys. However, these methods can be challenging due to the dense vegetation and the fact that mangroves grow in hard-to-reach intertidal zones. On top of that, field surveys are often labor-intensive, expensive, and usually cover only small areas. Remote sensing (RS) has addressed the limitations of traditional field surveys, offering an easier and effective way to monitor mangroves. RS is a popular technique for mapping mangrove extents. It offers a more inexpensive alternative than on-the-ground techniques. Satellite imagery from sources like Sentinel and Landsat is readily available and free [4]. Additionally, images from past years are stored, making it easy for researchers to analyze and monitor significant changes in the distribution and covering of mangrove forests over time [7].

To distinguish mangrove from other types of land cover and vegetation, researchers have created indices to accurately map their extent. Spectral indices combine pixel values from two or more bands in a multispectral image. They are designed to highlight areas that show the presence or absence of specific land-cover types in the image [8]. The use of thresholds on spectral indices helps classify different land cover types or features more effectively. By setting a specific threshold value, researchers can separate certain features like vegetation, water, or mangroves from other land covers in satellite imagery. However, the specific threshold value for identifying mangroves in a spectral index varies depending on the index used, the geographic region, and the quality of the satellite imagery. A study of Baloloy [7], attests to the potential of threshold segmentation-based indices, pointing out that they are easier to use, quicker, and less skill-intensive than classification procedures [9][10]. With this, the proponents would like to introduce a percentile-based threshold segmentation technique, by identifying the optimal threshold value of the mangrove index, to differentiate spectral properties of different classes in the imagery. One of the main goals of the indices is to accentuate the spectral properties of the target class to deviate from other classes.

The present study aims to (i) to classify and map mangrove extent by utilizing the percentile-based threshold segmentation technique.; (ii) to identify growth trends and forecast future changes of mangrove cover in Eastern Leyte between the years 2017 to 2023 using satellite images; and (iii) to assess the accuracy of the proposed method with ground truth data.

## DATA AND STUDY AREA

### Study Area

The study area (Figure 1) is situated in Leyte province, Eastern Visayas, Philippines, covering the municipalities of Tacloban City, Palo, and Tanauan. Bordered by Alangalang, Dulag, Tolosa, and the Leyte Gulf, this area spans approximately 2,367 square kilometers. The coordinates for the key locations within the study area are Tacloban City (11°7'N, 124°59'E), Palo (11°4'N, 124°56'E), and Tanauan (11°0'N, 124°55'E). The region features diverse topography, ranging from sea level to around 1,000 meters above sea level, with mountainous areas, coastal plains, and river valleys. A tropical monsoon climate, characterized by distinct wet and dry seasons, influences the local environment and vegetation patterns.

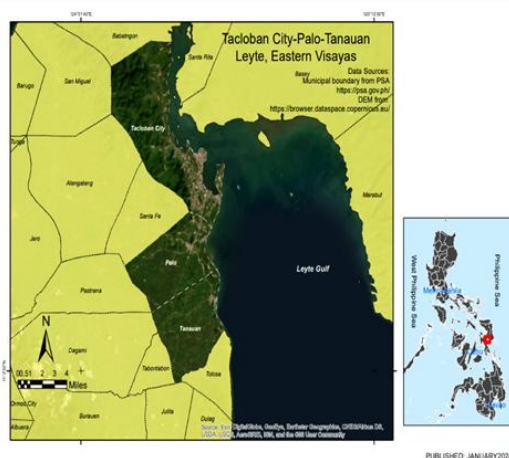


**Figure 1.** The Study Area – Tacloban City, and the Municipalities of Palo and Tanauan Leyte

Significant features include the Leyte Gulf, which borders the eastern side of the area, and the San Juanico Strait to the north, which connects the Leyte Gulf to the Philippine Sea. The Leyte National Park, located in the northern part of the region, adds ecological value to the area by supporting conservation efforts and protecting biodiversity. These geographic and environmental characteristics make this region well-suited for studying mangrove dynamics, as it demonstrates the interaction between terrestrial and marine ecosystems, influenced by both climate and topography.

### Satellite Data

The study utilizes two types of satellite imagery: data acquired from Sentinel-2A and imagery provided by ESRI, that serve as the validation dataset.

The first image data was obtained from the Sentinel-2 MultiSpectral Instrument (MSI), which is part of the Copernicus program operated by the European Space Agency (ESA). Sentinel-2 satellite imagery was utilized for mangrove mapping due to its high spatial and spectral resolution. The dataset was obtained from the Copernicus Open Access Hub, covering the study area with a spatial resolution of 10 meters. The Sentinel-2A MSI provides high-resolution optical imagery in 13 spectral bands, ranging from the visible and near-infrared to the short-wave infrared parts of the electromagnetic spectrum. The selected bands included visible near-infrared (NIR) 0.842  $\mu\text{m}$ , and shortwave infrared (SWIR) 1.161  $\mu\text{m}$ , and Green with 0.560  $\mu\text{m}$ , which are effective in distinguishing mangrove vegetation from other land cover types [10]. Spectral bands refer to specific ranges of wavelengths in the electromagnetic spectrum that are measured by a sensor such as a satellite or airborne instruments [11]. Each spectral band captures information about the reflectance or emission properties of the Earth's surface within that specific wavelength range [12]. These bands are essential for various applications, including monitoring vegetation, soil, water bodies, and coastal areas (Table 1).

**Table 1.** Spectral Bands for Sentinel-2A Sensors

Band Number	Central Wavelength (nm)	Bandwidth (nm)	Spatial Resolution (m)
1 (Coastal Aerosol)	442.7	20	60
2 (Blue)	492.7	65	10
3 (Green)	559.8	35	10
4 (Red)	664.6	30	10
5 (Red Edge 1)	704.1	14	20
6 (Red Edge 2)	740.5	14	20
7 (Red Edge 3)	782.8	19	20
8 (NIR)	832.8	105	10
8a (Narrow NIR)	864.7	21	20
9 (Water vapor)	945.1	19	60
10 (SWIR – Cirrus)	1373.5	29	60
11 (SWIR1)	1613.7	90	20
12 (SWIR2)	2202.4	174	20

Another data utilized in this study was sourced from Environmental Systems Research Institute (ESRI) platform provides a comprehensive dataset for geographic information system (GIS) analysis. This dataset are images from 2017 to 2023 which contains detailed classifications of land cover types such as forests, agricultural zones, urban areas, and water bodies. The ESRI imagery served as the validation data and comparison for assessing the below and above 75% threshold of the Mangrove index (MI) values.

### Ground Truth Data

To evaluate the spatial distribution of mangroves in the Eastern Leyte study area, a field observation was carried out from April to June 2024. A stratified sampling method was utilized to ensure that all relevant sub-areas within the study site were adequately represented. To facilitate this, a grid with evenly spaced points was created across the

entire study area, maintaining a uniform interval of 10 meters between points. These points are randomly selected for accuracy assessment.

Acquiring ground-truth data for validating the classified mangrove extent posed a challenge throughout the study. One significant issue was the inaccessibility of certain mangrove areas, particularly those located in remote, swampy, or flood-prone zones that were difficult to reach, especially during high tide or adverse weather conditions. To address this, the field validation was focused on accessible sites near roads and coastal barangays, with visits scheduled during low-tide windows.

A mobile GPS device was used to record the locations and to gather coordinates of the mangrove boundaries during the field surveys. These coordinates were subsequently compared with satellite data.

## METHODOLOGY

The workflow of this study is shown in Figure 2. The process begins with the acquisition of Sentinel-2A satellite imagery, which undergoes preprocessing procedures including atmospheric correction and cloud masking to ensure data quality. Spectral indices tailored for vegetation detection are then calculated to enhance the distinction of mangrove features. A thresholding technique is subsequently applied to classify mangrove and non-mangrove areas. To assess the accuracy of the classification, the outputs are validated against high-resolution reference imagery sourced from ESRI.

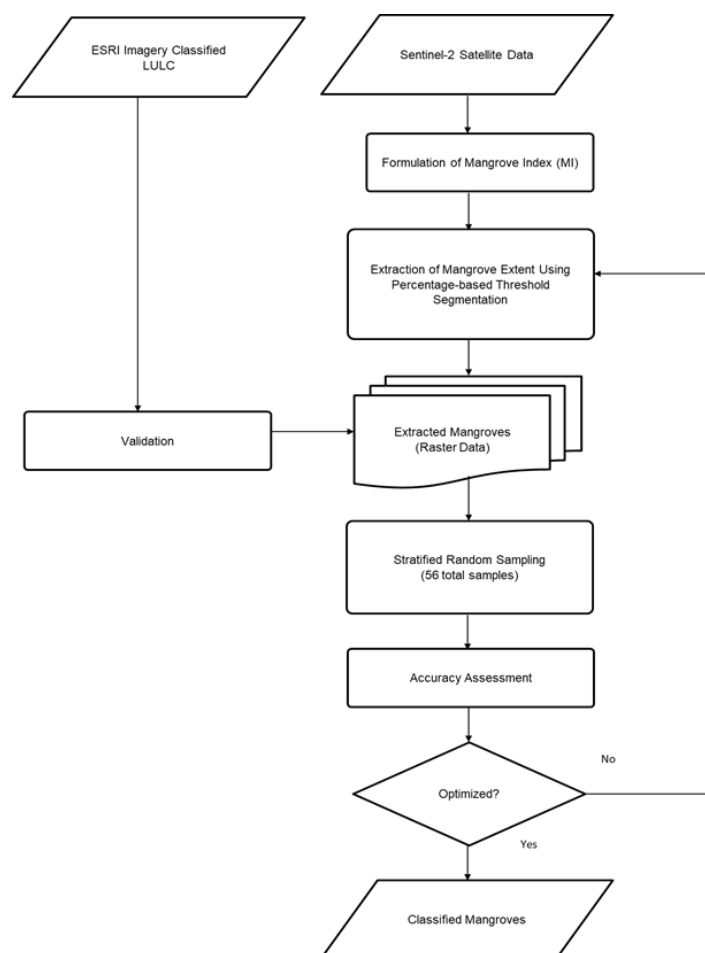


**Figure 2.** The Workflow of the Study

### Collection and Pre-processing of Sentinel-2A Data

The Sentinel-2A Multispectral Imager Instrument (MSI) Level 1-C images from 2017 to 2023 covering Tacloban City, Municipality of Palo and Tanauan, Leyte were downloaded from Copernicus Data Space. The image data has



undergone pre-processing. The preprocessing steps of the image data includes atmospheric correction and cloud masking. These are applied to enhance data quality and minimize distortions caused by atmospheric interference.

Cloud masking in Sentinel-2 Level-2A imagery is performed using the Scene Classification Layer (SCL) generated by the Sen2Cor processor to detect and mask pixels affected by clouds, cirrus, and cloud shadows. This is done using spectral information from key bands: visible bands like Band 2 (Blue), Band 3 (Green), and Band 4 (Red) are used to detect bright clouds due to their high reflectance. Thin cirrus clouds are identified using Band 10 (Cirrus), which is highly sensitive to atmospheric water vapor (Figure 3). Sen2Cor transforms Top-of-Atmosphere (TOA) reflectance to Bottom-of-Atmosphere (BOA) reflectance and classifies pixels into surface types using these wavelengths. Pixels labeled as cloud (classes 6–8) or cloud shadow (class 9) are excluded from analysis. This masking ensures that only clear-sky pixels are used for reliable applications like vegetation monitoring and land cover classification.

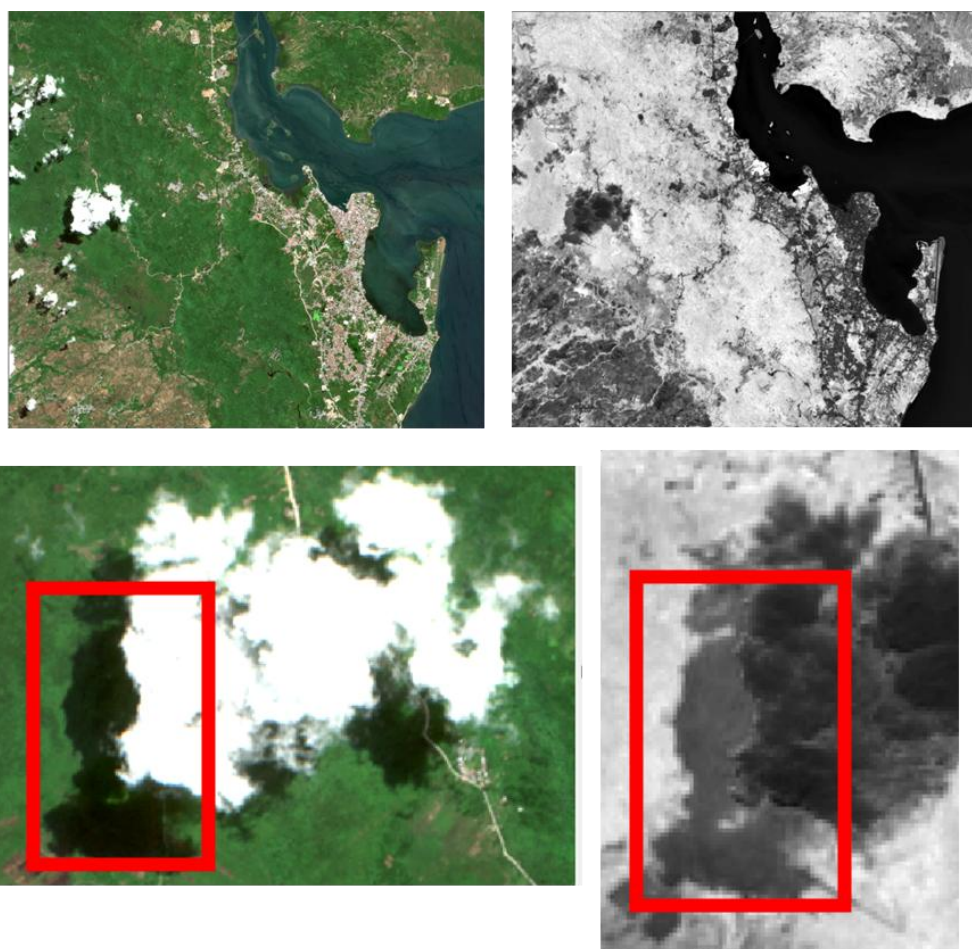


**Figure 3.** Cloud Masking in Sentinel-2A

### **Mangrove Index (MI)**

The Sentinel-2A spectral bands that were utilized in this study are: NIR, SWIR1, and Green wavelengths. The formula used is:

$$MI = \frac{NIR - Green}{SWIR1 + Green} \quad (1)$$

The formula is based on the study of Baloloy et al (2020) [7] which is the Mangrove Vegetation Index (MVI). The Mangrove Vegetation Index (MVI) utilizes three key spectral bands from Sentinel-2 imagery to enhance the detection of mangrove forests. The Near-Infrared (NIR) band (B8, 0.842  $\mu\text{m}$ ) captures strong reflectance from healthy vegetation, including mangroves, making it a crucial indicator of vegetation vigor. The Green band (B3, 0.560  $\mu\text{m}$ )

plays a significant role in vegetation differentiation by capturing reflectance from plant chlorophyll, aiding in distinguishing mangroves from other land cover types. Additionally, the Shortwave Infrared (SWIR) band (B11, 1.161  $\mu\text{m}$ ) is particularly useful for identifying vegetation moisture content and further differentiating mangroves from other vegetation types due to its sensitivity to water absorption characteristics. The combination of these bands in the MVI formula enhances the accuracy of mangrove extent mapping by leveraging their unique spectral properties.

Based on related studies on mangrove vegetation properties and their spectral responses, the SWIR and NIR bands were found to be effective in characterizing water absorption in vegetation and vegetation greenness, respectively [13].

### Percentile-Based Thresholding

As per the study conducted by Tran et. al. [14], there is no notably specific optimal threshold for the Mangrove Vegetation Index which differs from ranges of other classes. Hence, for this study, the MI values were analyzed. A series of threshold values for the mangrove index, ranging below and above 75% were evaluated. For each threshold, classification accuracy was utilized: Precision, Recall, and F1-score, based on a comparison with ground-truth data. The threshold value that achieved the highest overall accuracy was selected as the optimal threshold, enhancing the reliability of the mangrove extent mapping.

### Accuracy Assessment

The extracted mangrove data was validated by comparing with the land cover data from ESRI. Values generated in the distribution is extracted from the Mangrove spectral index.

The confusion matrix (Figure 4) is used to assess and evaluate the performance of the mangrove classification model. For each threshold value of mangrove index ranging above and below 75% were evaluated, and classified maps are generated. The accuracy of each map is measured by comparing it to a ground-truth dataset. Figure 3 shows a sample confusion matrix to evaluate the different thresholds.

		PREDICTED	
		MANGROVE	NON - MANGROVE
ACTUAL	MANGROVE	22 (TRUE POSITIVE)	4 (FALSE NEGATIVE)
	NON - MANGROVE	5 (FALSE POSITIVE)	25 (TRUE NEGATIVE)

**Figure 4.** The Confusion matrix

*True Positive (TP)* are mangroves correctly identified as mangroves by the model.

*True Negative (TN)* are non-mangroves correctly identified as non-mangroves by the model.

*False Positive (FP)* are mangroves incorrectly identified as non-mangroves by the model

*False Negative (FN)* are non-Mangroves incorrectly identified as mangroves by the model.

To implement the accuracy matrix, stratified random sampling was applied to the selected points for both mangrove and non-mangrove classes, with a total of 56 samples. The sample size of 56 points were selected to balance statistical reliability with available resources and time. In stratified sampling, the population is divided into distinct subgroups



$$Precision = \frac{TP}{TP + FP} \quad (4)$$

Recall (or Sensitivity) measures the proportion of correctly identified positive results out of all actual positives (Equation 5).

$$Recall = \frac{TP}{TP + FN} \quad (5)$$

F1 Score is the harmonic mean of Precision and Recall, giving a single score that balances both (equation 6).

$$F1\ Score = 2 \times \frac{Precision \times Recall}{Precision + Recall} \quad (6)$$

## RESULTS AND DISCUSSION

### The Optimal Threshold Value

To optimize classification accuracy, a series of threshold values for the mangrove index was explored, ranging below and above 75%. For each threshold, classification accuracy was evaluated using Overall Accuracy, Precision, Recall, and F1-score, and Kappa coefficient based on a comparison with ground-truth data. The threshold value that achieved the highest overall accuracy was selected as the optimal threshold, enhancing the reliability of the mangrove extent mapping.

**Table 2.** Comparison of the result of the accuracy matrix of Mangrove Index percentage-based threshold

Threshold (Percentage)	OA	Precision	Recall	F1 Score	Kappa
65%	66.1	67.9	65.5	66.7	0.32
70%	73.21	75.0	72.41	73.68	0.46
75%	83.93	86.21	83.33	84.75	0.68
80%	80.36	79.31	82.14	80.70	0.61
85%	78.57	76.92	76.92	76.92	0.57

Table 2 presents the performance metrics of different percentage-based thresholds models for classifying mangrove indices.

At the 65% threshold, the model shows moderate performance, with an Overall Accuracy of 66.1%. Precision (67.9%) slightly exceeds Recall (65.5%), indicating that the model is somewhat better at avoiding false positives than it is at identifying all true positives. However, the F1 Score of 66.7% and the Kappa value of 0.32 suggest only a slight agreement beyond random chance, indicating room for improvement.

Raising the threshold to 70% results in noticeable improvement. The model's accuracy increases to 73.21%, and both Precision (75.0%) and Recall (72.41%) are higher and more balanced, yielding a stronger F1 Score of 73.68%. The Kappa value also rises to 0.46, indicating better consistency and agreement.

The optimal performance is achieved at the 75% threshold, where the model reaches its highest accuracy of 83.93%. Precision (86.21%) and Recall (83.33%) are both strong, leading to a high F1 Score of 84.75%. The Kappa value of 0.68 reflects substantial agreement, suggesting this threshold balances the trade-off between false positives and false negatives effectively.



At the 80% threshold, the model's accuracy decreases slightly to 80.36%. While Recall (82.14%) improves marginally, Precision drops to 79.31%, resulting in a lower F1 Score of 80.70% and a Kappa of 0.61. This decline suggests that setting a higher threshold may cause the model to miss some true positives, affecting overall performance.

Finally, at the 85% threshold, the model's metrics decline further. Both Precision and Recall fall to 76.92%, and the F1 Score remains the same at 76.92%. The Overall Accuracy drops to 78.57%, and the Kappa value decreases to 0.57, indicating moderate agreement. This suggests that a very high threshold makes the model too conservative, reducing its ability to identify positive instances effectively.

In summary, the analysis indicates that the 75% threshold provides the best balance between Precision and Recall, leading to optimal overall performance. Lower thresholds (e.g., 65%) result in more false positives, while higher thresholds (e.g., 80% and 85%) increase the likelihood of missing true positives, making the model less effective. Thus, the 75% threshold is recommended for achieving the highest accuracy and agreement in the classification of mangrove indices.

### Mangrove Classification Accuracy

The box plots in Figure 5 shows the separability of mangrove and other classes. This illustrates the distribution of Mangrove Index (MI) values across different land cover types for the year 2017 to 2023, highlighting the contrast between mangrove and non-mangrove areas. It can be observed that MI showed consistent separability from the other classes, indicating the MI values exhibit greater than 75th percentile range of values. This suggests that mangroves possess a unique spectral signature or vegetation index, making them easily identifiable using remote sensing techniques.

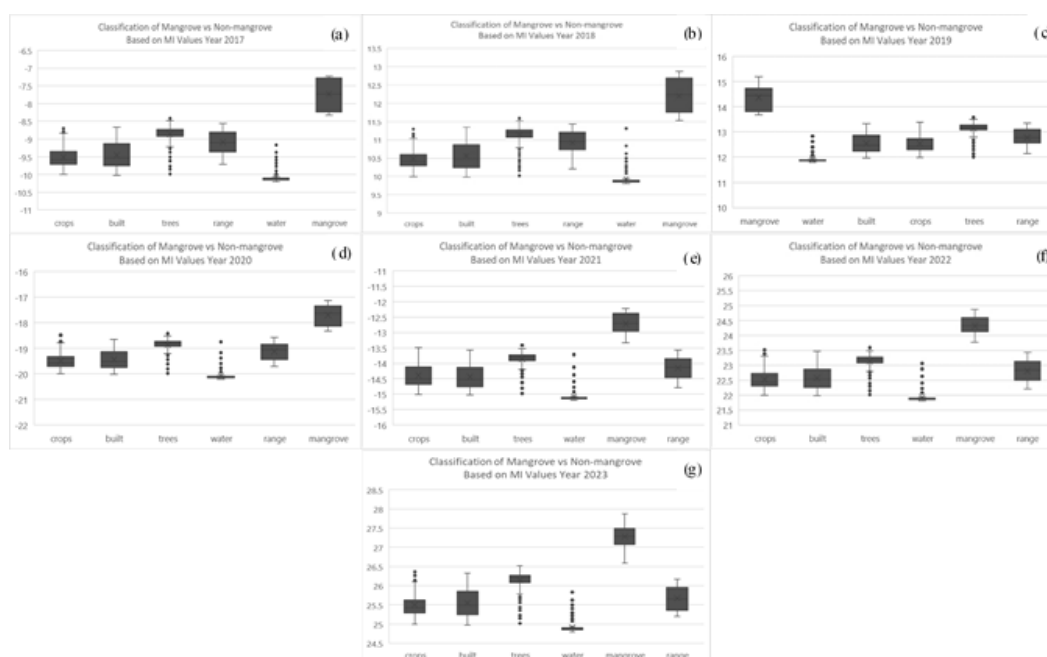


**Figure 6.** Mangrove Indices' Box plot values for each year. (A) 2017, (B) 2018, (C) 2019, (D) 2020, (E) 2021, (F) 2022, (G) 2023

### Mangrove Area Change

The calculation of the mangrove area was performed using Geographic Information System (GIS) software, specifically Zonal Statistics Tool in ArcGIS. The trend of mangrove area showed a steady growth over the period from 2017 to 2023 as shown in Table 3.

**Table 3.** Mangrove Area from 2017 to 2023

Year	Mangrove Area (ha)
2017	183.949
2018	321.382
2019	381.971
2020	417.158
2021	491.320
2022	544.178
2023	656.632

Figure 7 illustrates the changes in mangrove coverage in various municipalities of Leyte, Eastern Visayas, from 2017 to 2023 using Sentinel-2 MSI based on the >75% percentile of the Mangrove Index. It is observed that the mangrove area increased by approximately 256.96% from 2017 to 2023, growing from 183.949 ha to 656.632 ha.

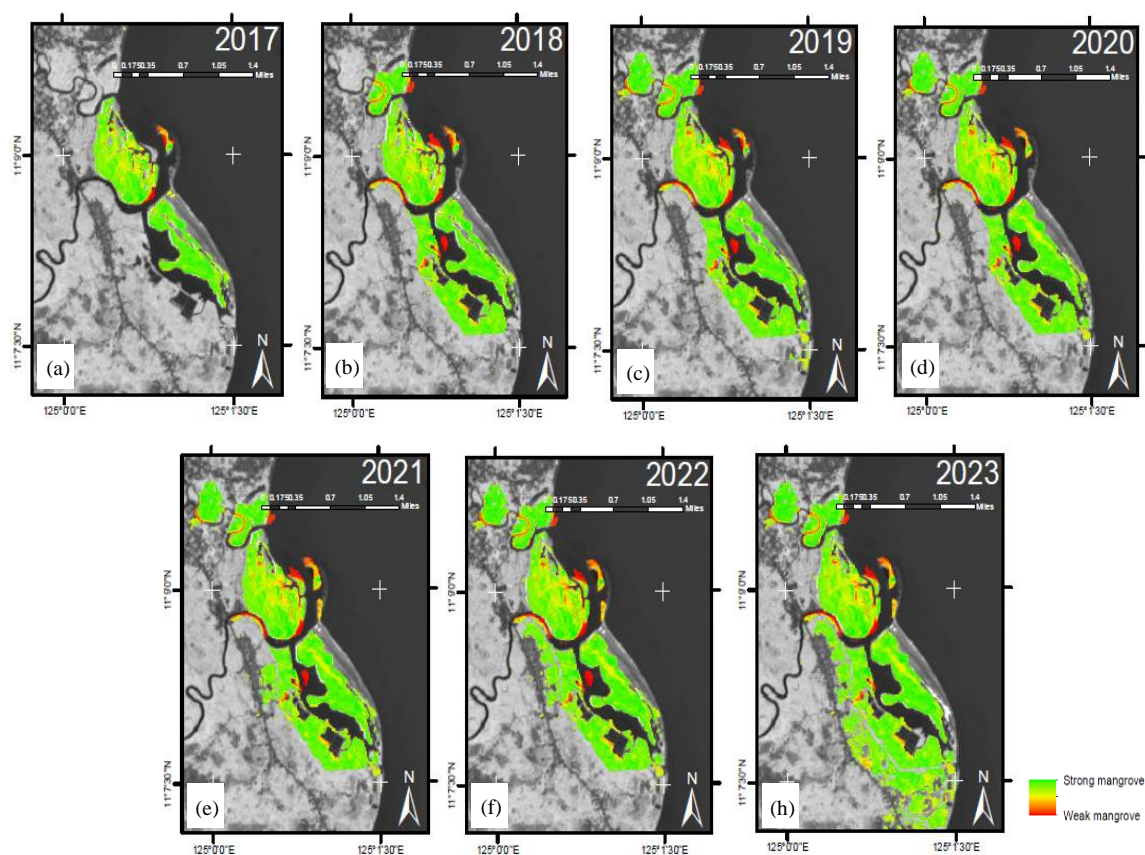


**Figure 7.** Images of the Change of Mangrove Extent from (a) 2017, (b) 2018, (c) 2019, (d) 2020, (e) 2021, (f) 2022 and (g) 2023 using the Mangrove Index (MI) with 75% threshold

### Mapping of Mangrove Extent using the Mangrove Index (MI)

Figure 8 illustrates the changes in mangrove coverage in various municipalities of Leyte, Eastern Visayas, from 2017 to 2023 using Sentinel-2 MSI based on the >75% percentile of the Mangrove Index.

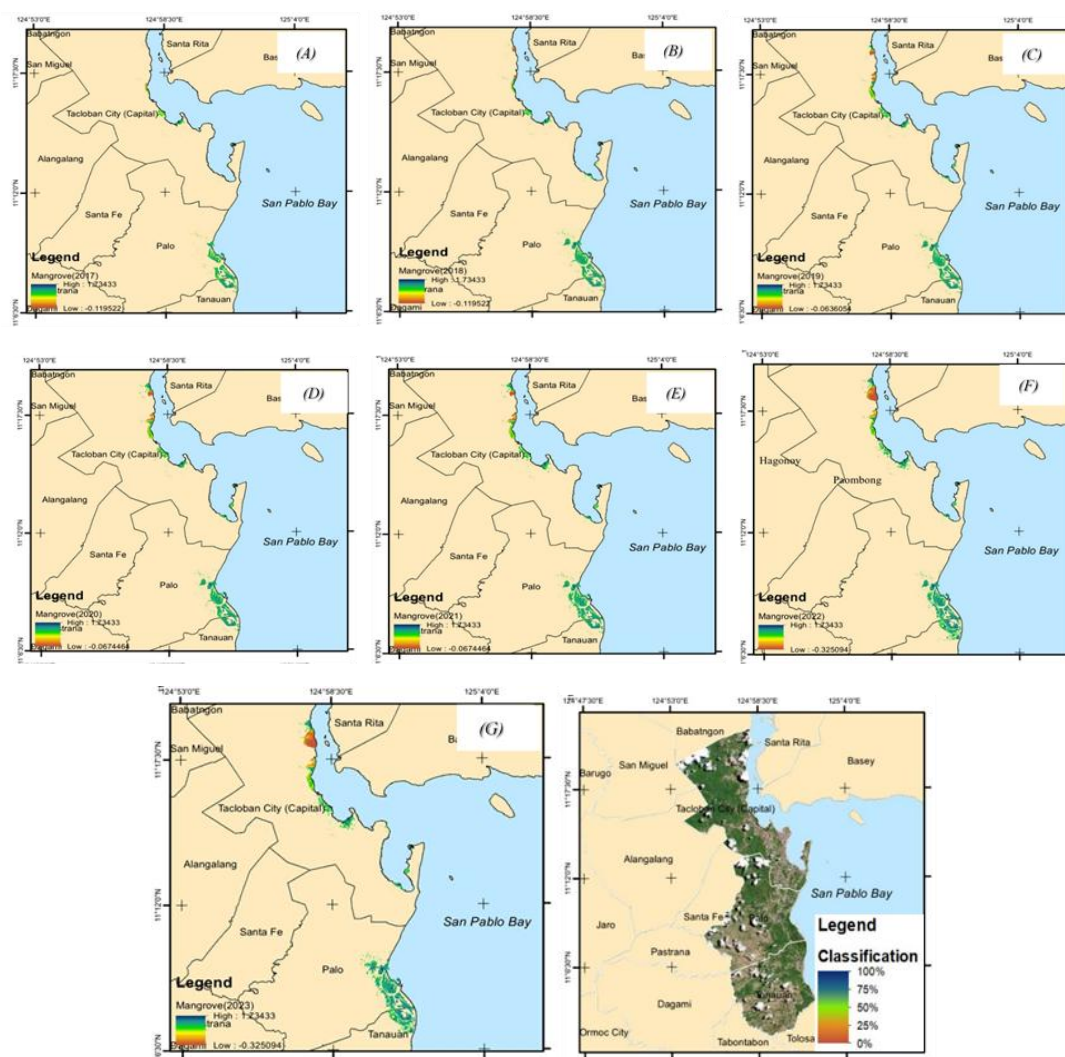


**Figure 8.** The Change of Mangrove Extent per Year from (a) 2017 (b) 2018 (c) 2019 (d) 2020 (e) 2021 (f) 2022 (g) 2023 and (h) the RGB Satellite Image Year 2024

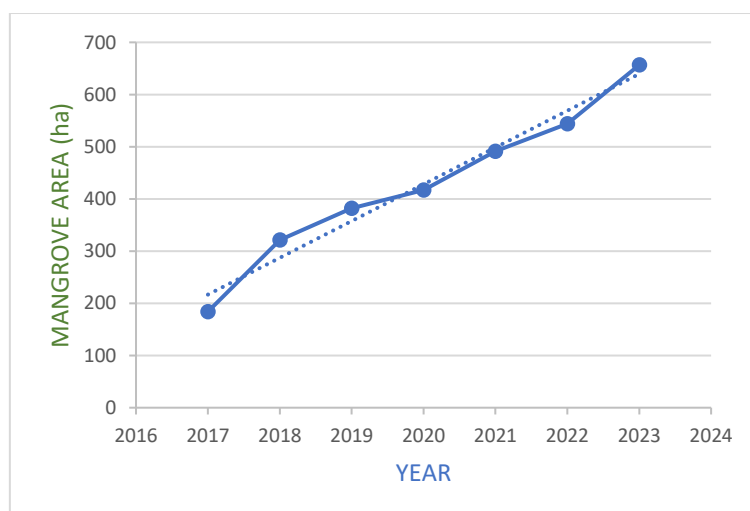


**Figure 9.** The trend in Mangrove Area Per Year

The satellite data shows a remarkable recovery and expansion of mangrove coverage in Eastern Leyte, following the destruction caused by Typhoon Haiyan in 2013.

The graph in Figure 9 illustrates the expansion of mangrove areas from 2017 to 2023, showing a general upward trend in coverage. In 2017, the mangrove area was recorded at 183.95 hectares. A significant increase of 74.71% occurred between 2017 and 2018, reaching 321.38 hectares. This rapid growth suggests that early post-disturbance factors, such as natural regeneration and possibly improved environmental conditions, may have played a role. However, from 2018 to 2019, the growth rate slowed to 18.85%, bringing the total area to 381.97 hectares.

In the following years, mangrove expansion continued at a more moderate pace, with a 9.21% increase from 2019 to 2020 (417.16 hectares) and a slightly higher 17.78% growth from 2020 to 2021 (491.32 hectares). From 2021 to 2022, the growth rate was 10.76%, reaching 544.18 hectares. From 2022 to 2023, the mangrove area saw a notable increase of 20.66%, reaching 656.63 hectares. This recent acceleration could indicate favorable ecological conditions, reduced disturbances, or the natural ability of mangroves to regenerate over time. While restoration efforts may have contributed, the variability in growth rates suggests that other factors, such as the resilience of pre-existing mangrove stands, hydrodynamic processes, and climate conditions, likely influenced the observed patterns. This aligns with the study of Cabello [4] emphasized that mangrove recovery after Typhoon Yolanda is not just about external restoration efforts, it is likely influenced by the pre-disturbance extent and ecological condition of the forest.

### Forecasting Future Change of Mangrove Extent

A time series analysis was performed on mangrove area data, utilizing historical trends to forecast future changes and estimate expected coverage in the coming years.

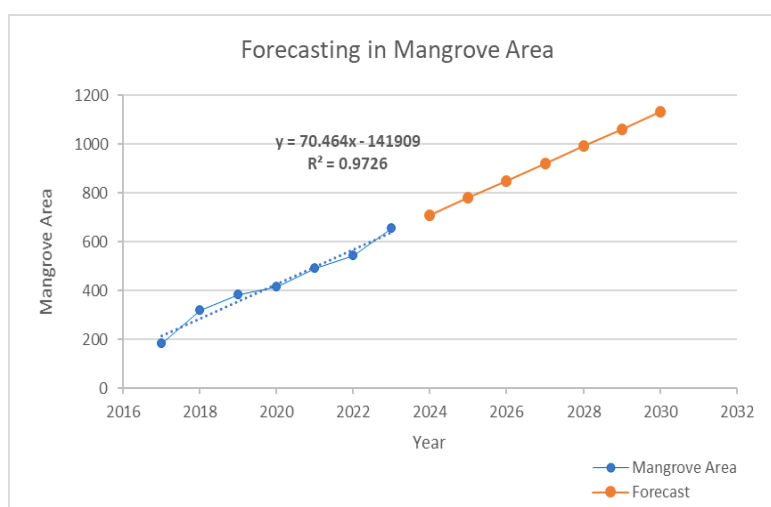


**Figure 10.** The trend in Mangrove Area Per Year

The graph presents a time series analysis of mangrove area growth from 2017 to 2023, with a forecast projecting this trend through to 2030. The blue dots and line represent the actual data collected over the years, showing a steady increase in mangrove coverage. The orange dots and line extend this trend into the future, giving an estimate of what the mangrove area might look like if the current growth pattern continues.

The trendline equation,  $y = 70.464x - 141909$ , suggests a consistent, steady increase in mangrove area over time. The high  $R^2$  value of 0.9726 indicates that this model fits the data well, it can explain about 97% of the changes observed in the historical data.

### CONCLUSION

This study demonstrates the effectiveness of using satellite images and percentile-based threshold segmentation of mangrove index methods to classify and detect mangrove areas in Eastern Leyte, Philippines. Mangroves are vital to the environment, providing shoreline protection, carbon storage, and habitats for marine life. Accurate mapping and monitoring are essential for their conservation and management.



The study employed a method based on 75th percentile thresholds to detect and classify mangrove areas, validated by field surveys that provided ground truth data. The classification results showed an overall accuracy rate of 83.93% and a Kappa coefficient of 0.678, indicating substantial agreement between the classified information and the actual data. The classification model performs well in distinguishing between mangrove and non-mangrove areas with high accuracy. The Precision and Recall show a strong model performance with 86.21% and 83.33% respectively. However, there is still room for improvement to achieve higher accuracy and reliability of the model. These results confirm that the percentile-based threshold segmentation method is a reliable tool for distinguishing mangrove areas from other land cover types using the Sentinel-2A satellite images.

### **CONFLICT OF INTEREST**

The authors declare no conflict of interest.

### **REFERENCES**

- [1] M. S. e. al., "Mangrove Canopy Height Globally related to precipitation, temperature and cyclone frequency," *Natural Geoscience*, vol. 12, no. 1, pp. 40-45, December 2018.
- [2] S. N. e. al., "The Effectiveness, Costs and Coastal Protection Benefits of Natural and Nature-Based Defences," *PLoS ONE*, vol. 11, no. 5, p. e0154735, 2016.
- [3] Philippine Atmospheric, Geophysical and Astronomical Services Administration, "Bagong Pagasa Website," [Online]. Available: <https://www.pagasa.dost.gov.ph/climate/tropical-cyclone-information>. [Accessed 2024].
- [4] Cabello, Germentil, Blanco, Macatulad and Salmo III, "Post-disaster assessment of mangrove forest recovery in Lawaan-Balangiga, Eastern Samar using NDVI time series analysis," *ISPRS Ann. Photogramm. Remote Sens. Spatial Inf. Sci*, vol. Vol 3, pp. 243-250, 2021.
- [5] Kirui, Kairo, Viergever, Rudra, Huxham and Briers, "Mapping of mangrove forest land cover change along the Kenya coastline using Landsat imagery," *Ocean & Coastal Management*, vol. 83, pp. 19-24, 2011.
- [6] Alatorre, Sánchez-Andrés, Cirujano, Beguería and Sánchez-Carrillo, "Identification of Mangrove Areas by Remote Sensing: The ROC Curve Technique Applied to the Northwestern Mexico Coastal Zone Using Landsat Imagery," *Remote Sensing*, vol. 3, no. Issue 8, 2011.
- [7] Baloloy, Blanco, Sta. Ana and Nadaoka, "Development and application of a new mangrove vegetation index (MVI) for rapid and accurate mangrove mapping," *ISPRS Journal of Photogrammetry and Remote Sensing*, vol. 166, pp. 95-117, 2020.
- [8] V. Vinay and J. L., "Introducing the Spectral Index Library in ArcGIS," [Online]. Available: <https://www.esri.com/about/newsroom/arcuser/spectral-library>. [Accessed June 2024].
- [9] C. D. C. Zablan, A. C. Blanco, K. Nadaoka, K. P. Martinez, and A. B. Baloloy, "ASSESSMENT OF MANGROVE EXTENT EXTRACTION ACCURACY OF THRESHOLD SEGMENTATION-BASED INDICES USING SENTINEL IMAGERY," *the International Archives of the Photogrammetry, Remote Sensing and Spatial Information Sciences/International Archives of the Photogrammetry, Remote Sensing and Spatial Information Sciences*, vol. XLVIII-4/W6-2022, pp. 391-401, Feb. 2023, doi: 10.5194/isprs-archives-xxviii-4-w6-2022-391-2023.
- [10] Prayudha, B., Ulumuddin, Y. I., Siregar, V., Suyarso, Agus, S. B., Prasetyo, L. B., Suyadi, Avianto, P., & Ramadhani, M. R. (2024). Enhanced mangrove index: A spectral index for discrimination understorey, nypa, and mangrove trees. *MethodsX*, 12(May), 102778. <https://doi.org/10.1016/j.mex.2024.102778>
- [11] NASA, "Multispectral Instrument (MSI)," *EarthData*, [Online]. Available: <https://www.earthdata.nasa.gov/sensors/sentinel-2-msi>. [Accessed 2024].
- [12] ESRI, "Sentinel-2 Land Cover Explore," [Online]. Available: <https://livingatlas.arcgis.com/landcoverexplorer/>. [Accessed 2024].
- [13] Wang, Wan, Qiu, Guo, Wang, Sun and Wu, "Evaluating the Performance of Sentinel-2, Landsat 8 and Pléiades-1 in Mapping Mangrove Extent and Species," *Remote Sensing*, vol. 10, no. 9, 2018.
- [14] Tran, Reef and Zhu, "A Review of Spectral Indices for Mangrove Remote Sensing," *Remote Sensing in mangroves II*, vol. 14, no. 19, 2022.